Eph receptor function is modulated by heterooligomerization of A and B type Eph receptors

Peter W. Janes,[1] Bettina Griesshaber,[1] Lakmali Atapattu,[1] Eva Nievergall,[1] Linda L. Hii,[1] Anneloes Mensinga,[1] Chanly Chheang,[1] Bryan W. Day,[2] Andrew W. Boyd,[2] Philippe I. Bastiaens,[3] Claus Jørgensen,[4] Tony Pawson,[4] and Martin Lackmann[1]

[1]Department of Biochemistry and Molecular Biology, Monash University, Victoria 3800, Australia
[2]Queensland Institute of Medical Research, Royal Brisbane Hospital, Brisbane, QLD, 4006 Australia
[3]Max Planck Institute of Molecular Physiology, 44227 Dortmund, Germany
[4]Samuel Lunenfeld Research Institute, Toronto, Ontario M5G 1X5, Canada

Eph receptors interact with ephrin ligands on adjacent cells to facilitate tissue patterning during normal and oncogenic development, in which unscheduled expression and somatic mutations contribute to tumor progression. EphA and B subtypes preferentially bind A- and B-type ephrins, respectively, resulting in receptor complexes that propagate via homotypic Eph–Eph interactions. We now show that EphA and B receptors cocluster, such that specific ligation of one receptor promotes recruitment and cross-activation of the other. Remarkably, coexpression of a kinase-inactive mutant EphA3 with wild-type EphB2 can cause either cross-activation or cross-inhibition, depending on relative expression. Our findings indicate that cellular responses to ephrin contact are determined by the EphA/EphB receptor profile on a given cell rather than the individual Eph subclass. Importantly, they imply that in tumor cells coexpressing different Ephs, functional mutations in one subtype may cause phenotypes that are a result of altered signaling from heterotypic rather from homotypic Eph clusters.

Introduction

Eph receptor tyrosine kinases (Ephs) and their cell-bound ligands (ephrins) direct cell navigation and topographic mapping of tissues during developmental patterning by controlling cell–cell adhesion and segregation (Klein, 2004; Lackmann and Boyd, 2008). Their important cell guidance functions are increasingly recognized in a wide variety of cancers, in which Ephs and ephrins function during tumor invasion, neoangiogenesis, and metastasis (Janes et al., 2008; Pasquale, 2010). For several Ephs, tumor suppressor roles in prostate, colon, and breast tumors have been previously described (Huusko et al., 2004; Batlle et al., 2005; Noren et al., 2006). EphB receptor-mediated cell segregation of colon cancer cells and surrounding epithelial cells contains tumor growth by preventing invasion into ephrin-B–expressing tissue layers (Clevers and Batlle, 2006; Cortina et al., 2007), and EphB2 mutation or epigenetic silencing is a prerequisite for tumor expansion and correlates with poorer patient outcomes. In addition to EphB2, gene array analyses for diagnostic somatic mutations identified several other Eph receptors, in particular EphA3 and EphA7, among the most frequently mutated genes in colorectal (Sjöblom et al., 2006) and lung (Ding et al., 2008) cancer. Here, the identified mutations often target protein regions, including the kinase domain, likely affecting Eph signaling and biological activity (Pasquale, 2010).

Eph receptors are structurally grouped into EphA receptors, preferentially binding glycophosphatidylinositol-linked A-type ephrins, and EphBs, binding transmembrane B-type

Correspondence to Martin Lackmann: Martin.Lackmann@monash.edu

A. Mensinga's present address is Dept. of Molecular Cancer Research, University Medical Center Utrecht, 3584 CG Utrecht, Netherlands.

C. Jørgensen's present address is the Section of Cell and Molecular Biology, Institute of Cancer Research, London SW3 6JB, England, UK.

Abbreviations used in this paper: ANOVA, analysis of variance; AP, acceptor peptide; CRD, cysteine-rich domain; diHcRed, divalent *Heteractis crispa* red; FLIM, fluorescence lifetime imaging microscopy; FRET, Förster resonance energy transfer; IP, immunoprecipitate; LBD, ligand-binding domain; PY, phosphotyrosine; SA, streptavidin; WB, Western blot; Wt, wild type.

The Rockefeller University Press $30.00
J. Cell Biol. Vol. 195 No. 6 1033–1045
www.jcb.org/cgi/doi/10.1083/jcb.201104037

ephrins (Gale et al., 1996). Within these subtypes, ephrin–Eph interactions are largely promiscuous, but there is limited cross-reactivity between subtypes. Known exemptions include EphA4 ligating A- and B-type ephrins and ephrin-A5 binding all EphA and some EphB receptors (Himanen et al., 2004). Unlike other receptor tyrosine kinases, Ephs require oligomerization by cell surface–tethered or preclustered soluble ephrins for transphosphorylation, downstream signaling, and biological responses (Davis et al., 1994; Stein et al., 1998).

In addition to ephrin-induced oligomerization, homotypic interaction between Eph receptors independent of ephrin ligation is essential for the assembly and lateral propagation of signaling clusters (Wimmer-Kleikamp et al., 2004). The recently elucidated molecular architecture of the ephrin-bound and nonbound EphA2 extracellular domain (Himanen et al., 2010; Seiradake et al., 2010) confirmed structure/function analyses indicating the Eph–Eph-binding interfaces within the ephrin-binding domain and the adjacent cysteine-rich domain (CRD; Lackmann et al., 1998; Wimmer-Kleikamp et al., 2004). Furthermore, recent evidence further suggests that, in addition to Eph–ephrin and Eph–Eph interactions, actomyosin contractile forces modulating the actin cytoskeleton may participate in Eph clustering (Salaita et al., 2010).

During developmental patterning, various Eph family members have overlapping expression profiles (Xu et al., 2000; Lackmann and Boyd, 2008), and the final position of migrating cells or axons is determined by the sum of the cell surface Eph receptors, which are competing for available ephrin targets in this expression domain (Reber et al., 2004). Considering the promiscuity of Eph–ephrin interactions, this emphasizes the relevance of Eph receptor coclustering for signaling outcomes, as demonstrated for EphB1 and EphB6 (Freywald et al., 2002) and for EphA3 and EphA4 (Marquardt et al., 2005). In these cases, formation of heterologous Eph clusters was rationalized by promiscuous ephrins cross-linking both Eph receptors. However, the observation that Ephs are effectively recruited into signaling clusters independent of ephrin tethering could suggest that coclustering and composite signaling might also occur with EphA and EphB receptors if expressed on the same cell surface. This would imply signaling outcomes determined by clusters that comprise members of both Eph subclasses rather than Ephs that directly interact with compatible ephrins.

Indeed, we demonstrate here for the first time that EphA and -B receptors, which are expressed on the same cell, assemble into common signaling clusters. We provide evidence for functionally relevant coclusters of EphB2 and EphA2 or EphA3 on a range of tumor cells, in which constitutive basal association between heterotypic Ephs is increased by agonist ligation. Selective clustering of one of the Ephs triggers cross-activation of the heterologous receptors, and their combined signal determines the downstream response to a given agonist, even to the extent that overexpression of a kinase-inactive EphA inhibits EphB signaling in a dominant-negative manner. Our findings may help to explain some of the disparate cellular responses to Eph/ephrin signaling that have been reported in various biological and cell biological systems (Holmberg and Frisén, 2002; Pasquale, 2005; Lackmann and Boyd, 2008) and are likely to have important implications in a tumor setting, where a range of Eph receptors are frequently coexpressed in the same tumor and where frequent somatic mutations affecting functional domains of certain Ephs may have more complex consequences than previously appreciated (Pasquale, 2010).

Results

EphA and EphB receptors associate and cross-phosphorylate

We demonstrated previously that, in addition to EphA receptors, preclustered ephrin-A5 binds and activates EphB2 (Himanen et al., 2004), providing circumstantial evidence for the notion of cooperative signaling from EphA3 and EphB2 receptors. We investigated this concept by transfecting HEK293 cells with combinations of GFP-tagged EphB2 and divalent *Heteractis crispa* red (diHcRed)–tagged EphA3 receptors (Janes et al., 2005), discernable by their different apparent molecular masses on Western blots (WBs; Fig. 1 A, bottom blot). The transfected cells were exposed to preclustered ephrin-A5-Fc, binding both receptors with comparable affinities (Himanen et al., 2004), or to IIIA4, an activating mAb with exquisite specificity for EphA3 (Vearing et al., 2005). As expected, anti-EphB2 WB analysis of protein G pull-downs of ephrin-A5–associated receptors from cell lysates confirmed EphB2 binding, irrespective of the presence of EphA3 (Fig. 1 A, top blot). Interestingly, the IIIA4 mAb also immunoprecipitated EphB2 but only from cells coexpressing EphA3, suggesting that this pull-down occurred via interaction between EphB2 and EphA3. Accordingly, WB analysis with antiphosphotyrosine (α-PY) antibodies showed that IIIA4 induced phosphorylation not only of diHcRed-EphA3 but also of GFP-EphB2, discernable by its apparent lower molecular mass on WBs (Fig. 1 A, middle blot).

Although use of IIIA4 to oligomerize EphA3 guaranteed that recruitment and activation of EphB2 observed in these experiments is initiated by ligation of EphA3, a corresponding α-EphB2 antibody, which would allow testing if EphB2 ligation also triggers coclustering and activation of coexpressed EphA3, is not available. We achieved selective oligomerization of EphB2 by engineering EphB2 containing an N-terminal biotin acceptor peptide (AP) tag (AP-EphB2), serving as a unique biotinylation site for the *Escherichia coli* biotin ligase (BirA; Howarth et al., 2005). Exposure of cells expressing selectively biotinylated Ephs to tetravalent streptavidin (SA) will tether these into complexes (Howarth and Ting, 2008) and effectively induces activation (Nievergall et al., 2010) and internalization (Janes et al., 2009). In the current experiments, we used SA-coated magnetic Dynabeads to cluster and activate biotinylated AP-EphB2 and to allow selective recovery of AP–Eph receptor complexes after cell lysis. WB analysis with α-PY–EphA3 antibodies showed increasing phosphorylation peaking 20 min after the addition of beads (Fig. 1 B). Despite some apparent cross-reactivity of the antibodies for PY-EphB2 (Fig. 1 B, rightmost lane), a markedly increased PY-Eph signal in cells coexpressing both receptors indeed suggests phosphorylation of EphA3 and EphB2. Furthermore, immunoblotting with

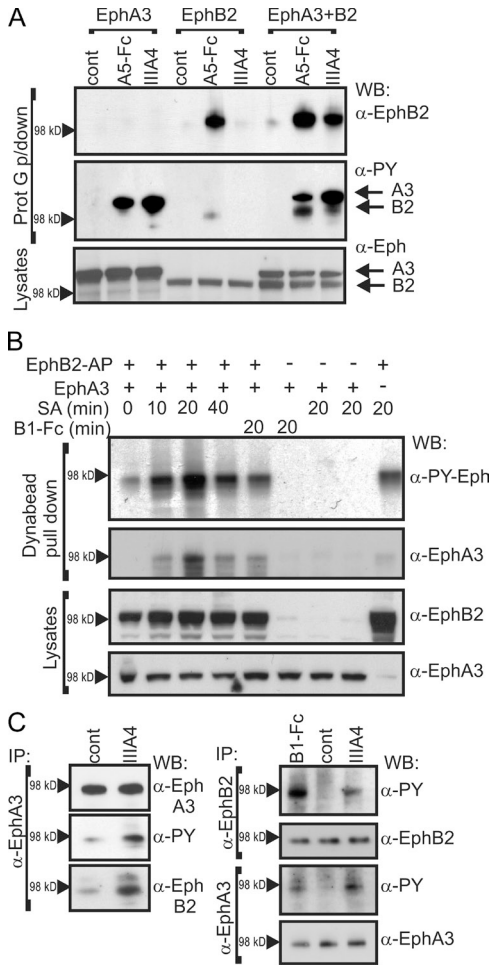

Figure 1. **EphA3 and EphB2 coIP from cells and are coactivated by receptor-specific stimulation.** (A) HEK293T cells transfected with diHcRed-EphA3 or GFP-EphB2 were stimulated for 15 min with ephrin-A5-Fc (A5-Fc), α-EphA3 mAb (IIIA4), or not stimulated (control [cont]). Ephrin or IIIA4-bound receptors were analyzed by a WB with the indicated antibodies. To control loading, lysates were blotted with α-EphA3 and α-EphB2 antibodies (bottom). Prot G p/down, protein G pull-down. (B) HEK293T cells transfected with EphA3 and/or with biotin ligase–treated AP-EphB2 were incubated with SA-coated Dynabeads for various times or with ephrin-B1-Fc/protein A Dynabeads as a control. Beads were recovered from cell lysates, and associated proteins were analyzed by a WB with α-EphA3 or α–PY-EphA3 antibodies. To control loading, total lysates were also blotted with α-EphA3 and α-EphB2 antibodies (bottom panels). (C) U251 glioma cells were treated with cross-linked IIIA4 and ephrin-B1-Fc to specifically activate EphA3 and EphB2, respectively, or left untreated (cont). (left) EphA3 IPs were immunoblotted for EphA3, PY, or associated EphB2. (right) Parallel EphB2 and EphA3 IPs were immunoblotted with α-EphA3, -EphB2, and -PY antibodies, as indicated.

α-EphA3 antibodies confirmed that increasing association between EphA3 and AP-EphB2 coincides with Eph activation. Some EphA3 is discernible also in immunoprecipitates (IPs) from cells transfected with AP-EphB2 alone (Fig. 1 B, rightmost lane), likely reflecting the moderate endogenous EphA3 expression found in HEK293T cells (Dottori et al., 1999).

Next, we determined whether coassociation between EphA and EphB receptors is possible in cells endogenously coexpressing both receptor classes. Screening of a range of tumor cell lines for EphA/B receptor coexpression revealed high levels of EphA3 and EphB2 in glioblastoma cell lines, including U251 cells. Likewise, quantitative RT-PCR of high-grade glioma patient samples showed frequent coexpression of EphA and EphB family members, indicating that their coexpression is prevalent in the primary cells and not a consequence of tissue culture (Fig. S1). Coimmunoprecipitation from U251 cells showed that IIIA4 treatment increased EphA3 activation and constitutive association with EphB2 (Fig. 1 C, left). Furthermore, α-PY WBs of EphB2 and EphA3 IPs from ephrin-B1-Fc and IIIA4-treated U251 cells (Fig. 1 C, right) indicate that both agonists trigger activation of EphA3 and of EphB2; more prominent phosphorylation in EphB2 IPs from ephrin-B1-Fc–stimulated cells and in EphA3 IPs from IIIA4-stimulated cells suggests preferential activation of either Eph by its specific agonist and coactivation of the other associated Eph receptor. In agreement, dissociation of EphB2 from α-EphA3 IPs prepared from ephrin-B1–stimulated U251 cells accordingly reduces the α-PY signal to intermediated levels above basal phosphorylation (Fig. S2 A), implying that both Ephs are coactivated during ephrin-B1 stimulation. Coclustering between EphAs and EphBs is also apparent in prostate cancer cells. LNCaP cells coexpress EphA3 and EphB2, and both receptors were coprecipitated from cell lysates with the α-EphA3 mAb (Fig. S2 B). In PC3 cells lacking detectable EphA3, but coexpressing EphA2 and EphB2, α-EphB2 IP antibodies revealed association between these two Ephs (Fig. S2 C). Together, these data support the notion that receptor coclustering likely occurs among various EphA and -B family members.

EphA and -B receptors associate in intact cells

To verify that EphA3 and EphB2 coclustering is not a consequence of cell lysis but occurs in intact cells, we analyzed Eph–Eph interactions by confocal microscopy in AP-EphA3/HEK293 cells that had been transfected with EphB2-GFP. Staining of intact cells with Alexa Fluor 594–tagged IIIA4 revealed noticeably colocalized GFP and Alexa Fluor 594 fluorescence on the cell surface, including on filopodia-like cell extensions (arrows and inset in top row of Fig. 2 A). To induce discernable localized clustering of AP-EphA3, we added SA-coated beads to these cells, prompting not only recruitment of biotinylated EphA3-AP but also of EphB2-GFP to the cell surface–attached beads (Fig. 2 A, bottom row).

Although clustering with SA-coated beads is efficient for activation of the biotinylated AP-EphA3, it does not allow endocytosis of activated receptors to proceed (Nievergall et al., 2010). To assess whether the two different Eph receptors are endocytosed within the same vesicles, we exposed GFP-EphB2 and diHcRed-EphA3–expressing cells to preclustered Alexa Fluor 647 IIIA4. Confocal microscopy revealed diHcRed-EphA3, Alexa Fluor 647 IIIA4, and GFP-EphB2 fluorescence colocalized in surface-proximal vesicles, likely representing early endosomes (Fig. 2 B, top row; Nievergall et al., 2010). Importantly, we observed colocalized endocytosis also in cells expressing kinase-inactive, PY signaling–defective EphB2[3YF] with phenylalanine substitutions at three regulatory tyrosine phosphorylation sites (Figs. 2 B [bottom row] and S3 A; Binns et al., 2000; Wybenga-Groot et al., 2001). In agreement, comparison

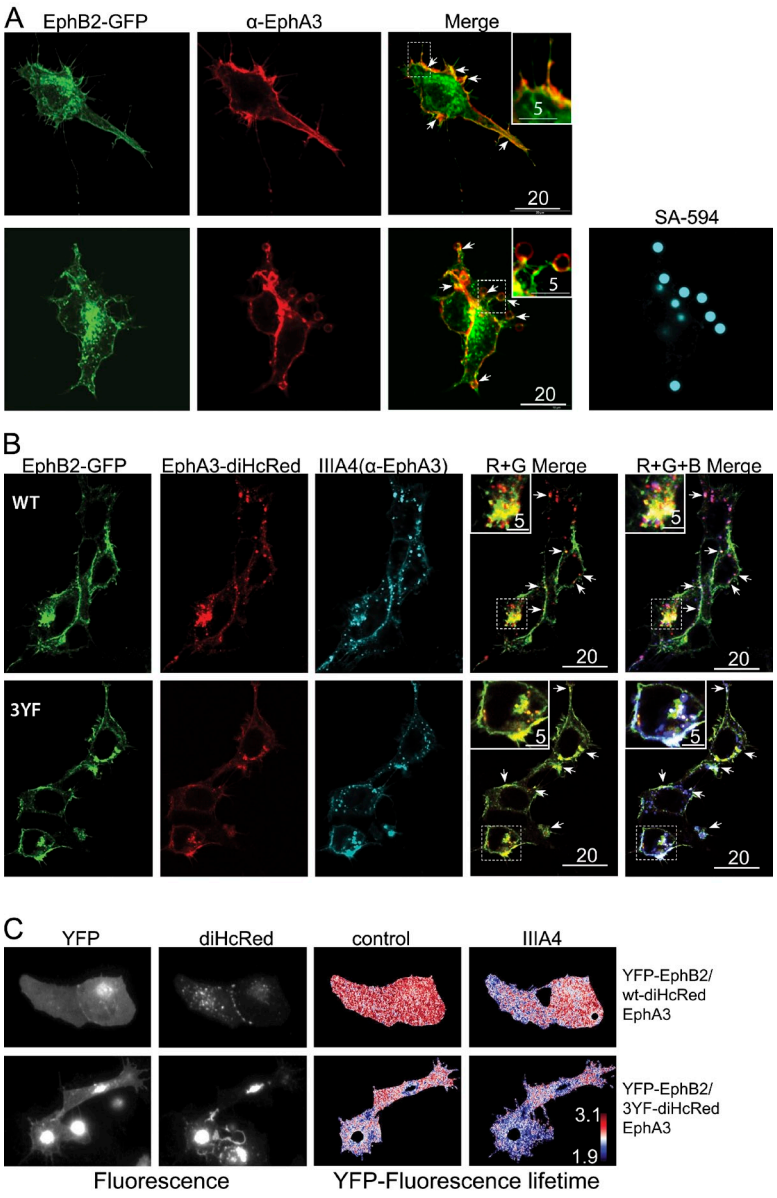

Figure 2. **Association of EphA3 and EphB2 in intact cells.** (A) Colocalization of AP-EphA3 and GFP-EphB2 in cells. HEK293 cells expressing biotinylated AP-EphA3 were transfected with GFP-EphB2. After 24 h, cells were stained with Alexa Fluor 647 α-EphA3 (IIIA4; red) before (top) or after (bottom) the addition of Alexa Fluor 594 SA–coated beads for 20 min, fixed, and imaged by confocal microscopy. (B) Cointernalization of EphA3 and EphB2. HEK293 cells were transfected with Wt diHcRed-EphA3 and Wt GFP-EphB2 or inactive mutant GFP-EphB2[3YF]. After 24 h, cells were stimulated for 20 min with cross-linked Alexa Fluor 647 IIIA4 before fixation and confocal microscopy. (A and B) Arrows indicate prominent colocalization. Insets show details in boxed areas at higher magnification. (C) Fluorescence lifetime microscopy shows close association of YFP-EphB2 and Wt or diHcRed-EphA3[3YF] in live cells. COS7 cells were transfected with YFP-EphB2 and Wt or 3YF mutant diHcRed-EphA3, and FRET between YFP and diHcRed was analyzed by FLIM before and after 40 min of stimulation with clustered IIIA4. YFP fluorescence lifetime maps are illustrated together with confocal micrographs of YFP-EphB2 and diHcRed-EphA3–transfected COS7 cells. All scale bars are in micrometers.

of IPs from cells expressing either wild-type (Wt) EphA3 and EphB2 or their tyrosine/phenylalanine substitution mutants confirmed coassociation between these Ephs, independent of their PY signal capacity (Fig. S3 B).

Next, we studied the suggested interaction between the EphA and EphB receptors at increased spatial resolution using fluorescence lifetime imaging microscopy (FLIM), an approach that monitors a 1–10-nm proximity (Wouters et al., 2001; Jares-Erijman and Jovin, 2003) of donor and acceptor fluorophores (in our case, EphB2-YFP and EphA3-diHcRed, respectively). Depending on their distance, Förster resonance energy transfer (FRET) from the donor (EphB2-YFP) to the acceptor (EphA3-diHcRed) results in decreased donor fluorescence lifetimes, indicated in the figures by blue color coding. In agreement with our other findings, YFP fluorescence lifetime maps of YFP-EphB2 and diHcRed-EphA3–cotransfected COS7 cells reveal substantial IIIA4-enhanced interaction between the two receptors (Fig. 2 C). Importantly, FLIM analysis also reveals close proximity between EphB2 and a signaling-inactive EphA3[3YF] mutant (Fig. 2 C, bottom row), corroborating that intracellular PY signaling is not required for the association between the two receptors. In control experiments, acceptor photobleaching resulted in complete abrogation of attenuated donor fluorescence lifetimes (Fig. S3 C), confirming FRET between closely adjacent fluorophore-tagged receptors as a basis for the observed short YFP lifetimes.

Next, we investigated the protein domains involved in heterotypic Eph clustering. Previously, we demonstrated homotypic oligomerization of EphA3 via extracellular domain interactions (Wimmer-Kleikamp et al., 2004) and, by structural analysis of full EphA2 exodomain, identified the Eph–Eph interaction interfaces within the ligand-binding domain (LBD) and the adjacent CRD (Himanen et al., 2010). Coprecipitation of EphB2 with Wt or truncated EphA2 indicated that deletion of the LBD resulted in almost complete loss of the EphB2 association, whereas CRD deletion had a lesser effect (Fig. 3 A).

In agreement, EphA3 mutants lacking the CRD and LBD show increasingly impaired association with EphB2 (Fig. 3 B). Interestingly, truncation of the whole EphA3 cytoplasmic domain also slightly affected heteroclustering with EphB2.

Eph heterooligomerization modulates signaling and cell retraction

To unambiguously assess whether Eph signaling outcomes are indeed determined by heterologous clusters of A and B family members, we tested whether muted signaling by the kinase-inactive EphA receptor can be rescued by coclustering with the kinase-active EphB receptor. We used COS7 cells with endogenous EphB2 expression, which respond to ephrin-B stimulation, with marked cell retraction and cytoskeletal collapse (Koolpe et al., 2005), for transfection either with Wt EphA3 or with a kinase-inactive ATP-binding site mutant, EphA3[K653M]. In cells expressing Wt EphA3, selective EphA3 activation with preclustered Alexa Fluor 594 IIIA4 resulted in rapid cell rounding and retraction (Fig. 4 A, middle row), whereas a neighboring cell with low or undetectable EphA3 remained relatively unaffected (Fig. 4 A and Video 1). In agreement, parental COS7 cells lacking EphA3 expression did not respond (Fig. 4 B), confirming that IIIA4 directly binds and clusters only EphA3 but not endogenous EphB2. Remarkably, cells expressing the mutant, kinase-inactive EphA3[K653M], responded in a similar manner (Fig. 4, A [bottom row] and B and Video 2), suggesting cooperative signaling via endogenous EphB2.

Next, we tested in HEK293 cells with low endogenous Eph expression whether coexpression of mutant EphA3[K653M] with EphB2 rescues phosphorylation of the kinase-inactive EphA3 receptor. Use of GFP-EphB2 allowed to unambiguously distinguish between the two Ephs of similar endogenous size in WBs. Cells transfected with varying amounts of each receptor were stimulated with IIIA4, and bound receptor complexes were recovered and probed with α-PY antibodies. As expected, kinase-dead EphA3[K653M] was not phosphorylated when expressed on its own, whereas coexpression with high levels of EphB2 caused its robust phosphorylation (second lane of the top blot in Fig. 4 C). Interestingly, increasing the relative level of EphA3[K653M] compared with Wt EphB2 altered the level of phosphorylation of both receptors, suggesting possible inhibition of EphB2 activation by high levels of kinase-inactive EphA3 relative to EphB2. Thus, we analyzed cells coexpressing overall constant levels of GFP-EphB2 and EphA3, the latter at decreasing ratios of Wt and EphA3[K653M]. As expected, maximal phosphorylation of EphA3 and EphB2 was increasingly attenuated at increasing ratios of EphA3[K653M] over Wt EphA3, so that only background phosphorylation remained in the absence of Wt EphA3 (Fig. 4 D, EphA3 Wt/KM, 0:3).

To further investigate this dominant-negative cross-inhibition of a coclustered family member by signaling-defective EphA3[K653M], we compared ephrin-B1–induced EphB2 activation in COS7 cells and in COS7 cells stably expressing either Wt EphA3 or mutant EphA3[K653M] (Fig. 5, A and B). Wt EphA3 increased ephrin-B1–induced EphB2 phosphorylation, consistent with cooperative signaling, whereas overexpression of kinase-dead EphA3[K653M] effectively ablated

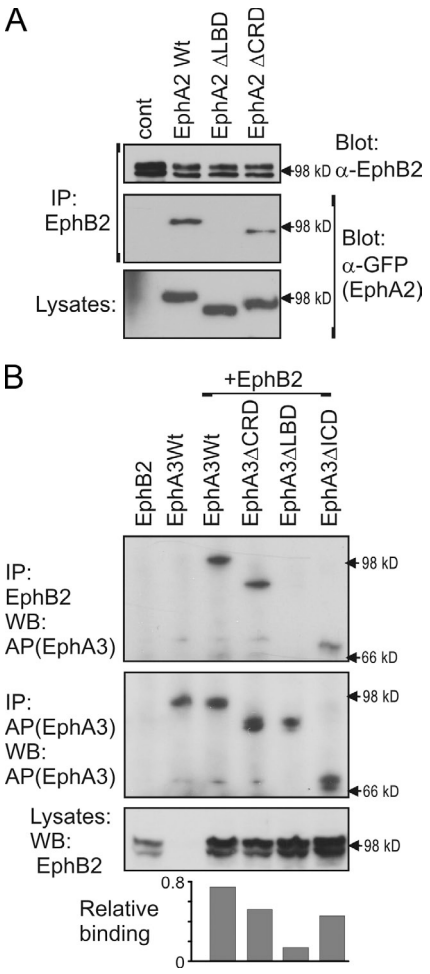

Figure 3. **Eph extracellular domains mediate heterooligomerization.** (A) HEK293T cells were transfected with Wt EphB2 alone (control [cont]) or with GFP-tagged EphA2 constructs, either full length (Wt) or lacking the ΔLBD or ΔCRD. EphB2 IPs were analyzed for associated GFP-EphA2 by an α-GFP WB and an α-EphB2 blot to confirm equal loading. Relative expression of GFP-EphA2 constructs was assessed by a WB of total cell lysates (bottom). (B) HEK293 cells were transfected with Wt EphB2 and AP-EphA3, full length (Wt) or lacking the ΔCRD, ΔLBD, or intracellular domain (ΔICD). EphB2 IPs were analyzed for associated AP-EphA3 by an α-AP WB. Relative expression of constructs was tested by an α-AP IP/WB and anti-EphB2 blots of total cell lysates. The graph shows relative EphA3 coIP/EphA3 expression from densitometry. A representative dataset from two independent experiments is shown.

EphB2 activation (Fig. 5 A, A3KM hi). In a parallel experiment, we confirmed that similarly high expression levels of Wt EphA3 notably enhanced ephrin-B1– as well as IIIA4-stimulated EphB2 activation, whereas, by comparison, COS7 cells expressing mutant EphA3[K653M] revealed strongly reduced EphB2 phosphorylation (Fig. 5 B).

Next, we investigated whether this dominant-negative inhibition of EphB2 activation by mutant EphA3 also translated into attenuation of Eph-induced cell morphology changes; indeed, whereas parental COS7 cells and a Wt EphA3–expressing COS7 line responded to ephrin-B1 with strong cell retraction, those with abundant EphA3[K653M] did not respond (Fig. 5, C and D; and Videos 3–6), with moderate retraction evident only in cells with low EphA3[K653M] expression (Video 6).

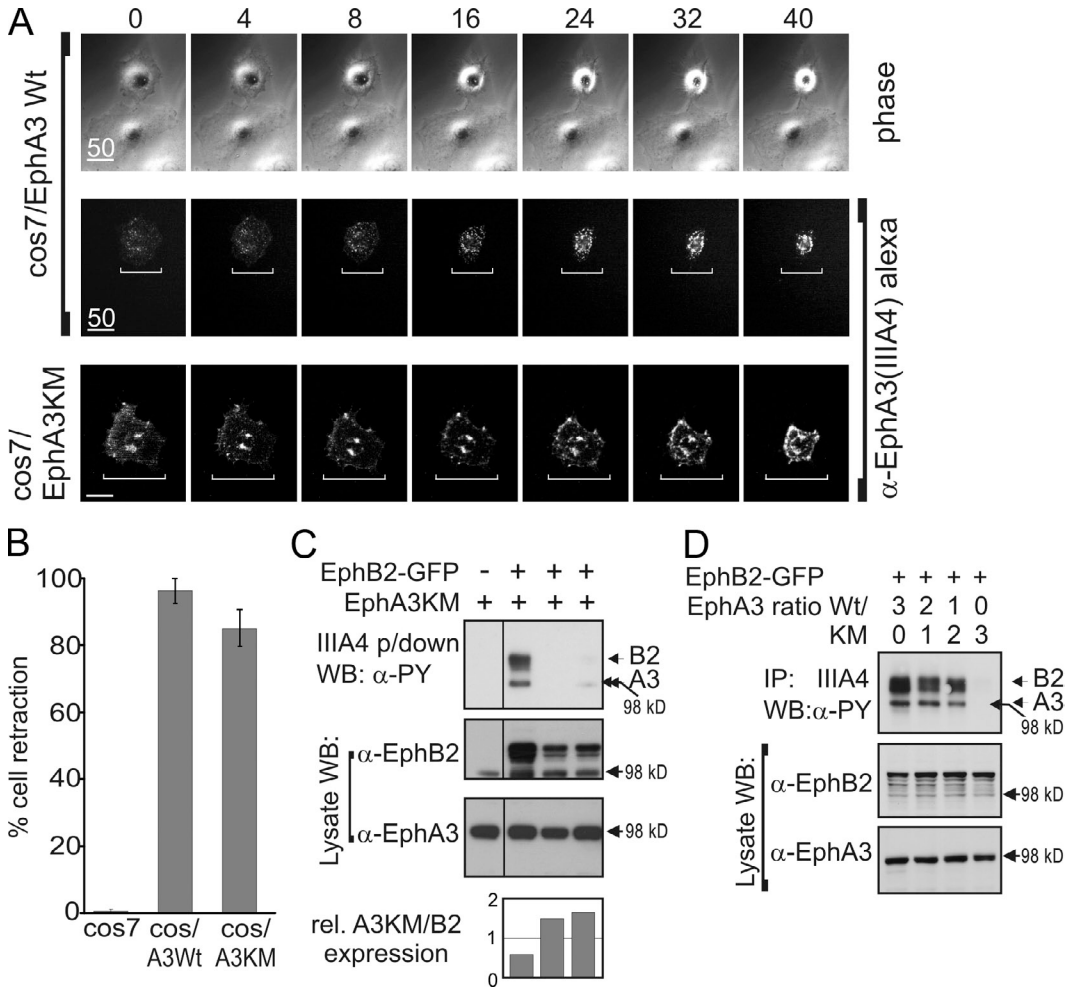

Figure 4. **Cross-activation of EphA3 and B2 can rescue an inactivated EphA3 receptor to induce cell retraction.** (A) Wt or EphA3[KM]-expressing COS7 cells were stimulated with Alexa Fluor 594–α–EphA3-mAb IIIA4 and imaged by brightfield (top row) and fluorescence (bottom rows) live-cell microscopy. Brackets in the fluorescent images depict cell diameters at the start of the experiment. The numbers above the images refer to time in minutes. All scale bars are in micrometers. (B) Quantification of parental COS7 or Wt- or EphA3[KM]-expressing cells retracting after IIIA4 stimulation, analyzed as in A (mean ± SEM; >90 cells/point from multiple fields). (C) Phosphorylation of EphA3[KM] by coexpression with EphB2. HEK293T cells, cotransfected with varying amounts of EphA3 (KM mutant) and GFP-EphB2, were stimulated with cross-linked IIIA4 and IIIA4-bound complexes analyzed by an α-PY WB. Antireceptor blots of lysates show relative expression levels, with irrelevant lanes removed. The graphs show relative EphA3/B2 (rel. A3KM/B2) expression from densitometry, using a representative dataset from two independent experiments. Black lines indicate that intervening lanes have been spliced out. p/down, pull-down. (D) Kinase-inactive EphA3 suppresses EphB2 activity. HEK293 cells transfected with constant levels of GFP-EphB2 and EphA3 (varying ratios of Wt to EphA3[KM], as indicated) and IIIA4-stimulated complexes were recovered on and Western blotted with α-PY antibodies. Cell lysates were also blotted for EphB2 and EphA3 as controls.

Modulation of cell segregation by Eph heterooligomers

To test cell biological consequences of Eph heteroclustering in a more physiological setting, we used a recently developed cell coculture system, modeling Eph/ephrin-mediated tissue boundary formation (Mellitzer et al., 1999) by monitoring segregation between Eph- and ephrin-expressing cells in 2D tissue culture (Poliakov et al., 2008; Jørgensen et al., 2009). Coculture of HEK293T cells expressing either ephrin-B1 or EphB2, the latter labeled with CellTracker green (Fig. 6) for ease of recognition, results in two distinct cell populations of green and unlabeled cells.

As expected, coculture with ephrin-B1–expressing cells results in tighter EphB2 colonies with brighter fluorescence intensity than what is seen in cocultures with parental HEK293T cells (Fig. 6 A, top two rows) with low endogenous ephrin expression (Nievergall et al., 2010). In contrast, cells expressing cytoplasmic-truncated EphB2ΔICD (Jørgensen et al., 2009) lose this ability and intermingle with ephrin-expressing cells. Thus, we tested whether the cell-sorting capacity of EphB2ΔICD cells could be rescued by coexpression of Wt EphA3, which has negligible affinity for ephrin-B1 (Lackmann et al., 1997). Indeed, in cocultures with ephrin-B1 cells, HEK293 cells stably expressing EphB2ΔICD together with EphA3 were clearly segregated into individual colonies (Fig. 6 A, fourth row). Furthermore, the ability for segregation of Wt EphB2 cells coexpressing EphA3 was notably increased relative to parental EphB2/HEK293 cells. By comparison, control HEK293 clones stably expressing only EphA3 segregated marginally from ephrin-B1 cells, confirming that direct ephrin-B1–EphA3 interactions contribute little to the segregation ability of EphB2ΔICD/EphA3 cells but

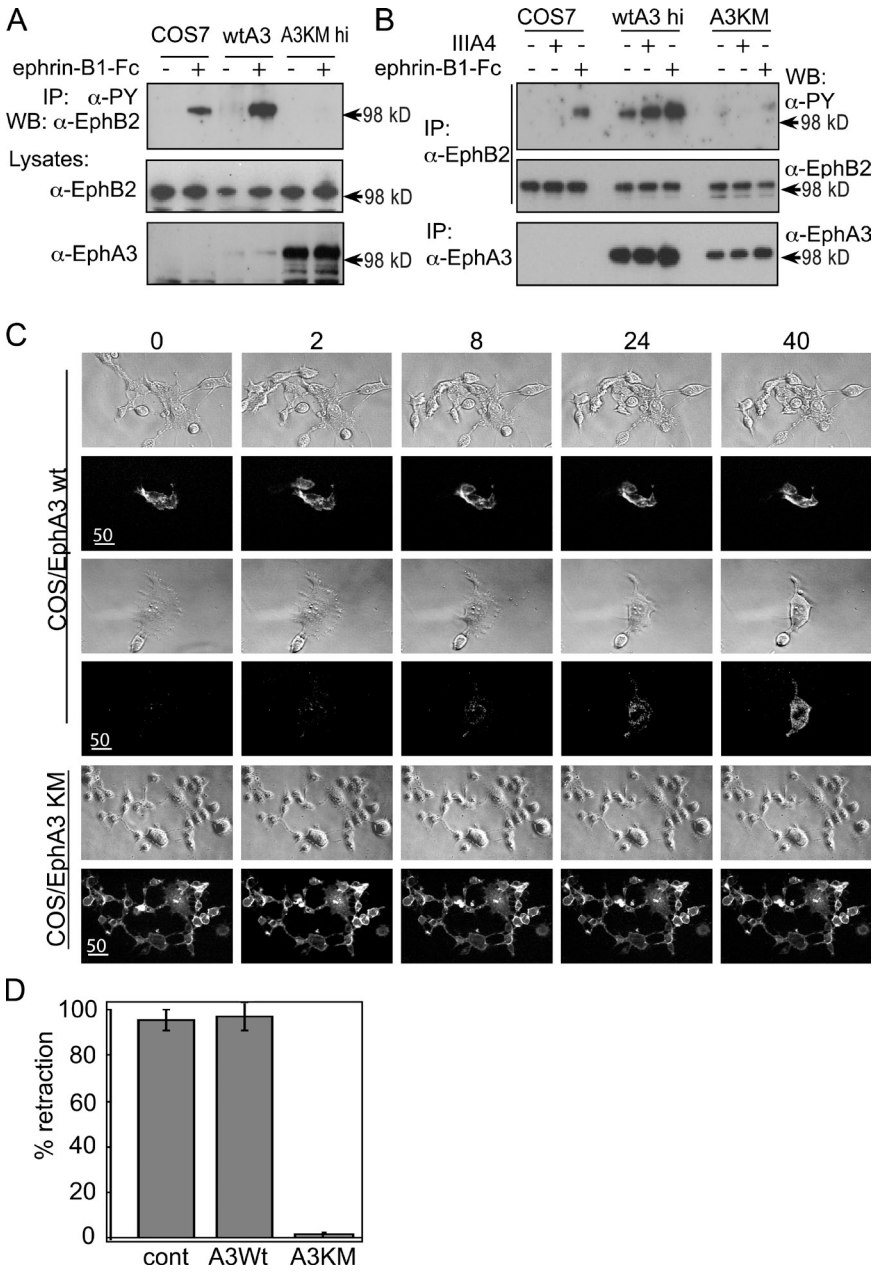

Figure 5. **Overexpression of kinase-dead EphA3 blocks EphB2 activation and cell retraction.** Comparison of EphB2 phosphorylation in Wt EphA3 and EphA3[KM] COS7 cell lines. (A) Parental COS7 cells (COS7) and clones stably expressing Wt EphA3 (wtA3) or high levels of K653M-EphA3 (A3KM hi) stimulated for 15 min with ephrin-B1-Fc were lysed, and α-PY Sepharose (4G10) IPs were analyzed by an α-EphB2 WB. α-EphA3 and α-EphB2 blots from total cell lysate antibodies show relative receptor expression levels. (B) Parental COS7 cells and clones stably overexpressing high levels of Wt EphA3 (wt EphA3 hi) or moderate levels of EphA3[KM] were stimulated with ephrin-B1-Fc or IIIA4, and α-EphB2 and -EphA3 IPs were Western blotted for EphB2 phosphorylation and Eph receptor expression levels, as indicated. (C) Ephrin-B1–induced cell retraction is blocked by exogenous kinase-dead EphA3. COS7 cells overexpressing Wt EphA3 (top four rows) or EphA3[KM] (bottom two rows) were labeled with (noncross-linked) Alexa Fluor 594 IIIA4 to indicate EphA3 expression, stimulated with cross-linked ephrin-B1-Fc, and analyzed by time-lapse fluorescence live-cell imaging. Cell retraction is imaged in a group of three cells that are part of a larger cell cluster (top two rows) and also in a single EphA3 Wt–expressing cell demonstrating more pronounced cell contraction (middle two rows). The numbers above the images refer to time in minutes. All scale bars are in micrometers. (D) The percentage of retracting cells with detectable EphA3 expression was quantified from B and compared with levels of parental COS7 cells (mean ± SEM; $n > 3$). cont, control.

that EphA3 is recruited into the ephrin-B1/EphB2ΔICD cluster and, upon cross-activation, relays the signal for segregation. Consistent with this, α-PY WBs of IPs from ephrinB1-Fc–treated EphB2ΔICD/EphA3 and Wt EphB2/EphA3 cells reveal greatly enhanced phosphorylation of EphA3 relative to control HEK293 cells expressing EphA3 alone (Fig. 6 C). Interestingly, in EphA3/HEK293 cells exposed to ephrin-B1/HEK293 cells instead of ephrin-B1-Fc, a small amount of EphA3 phosphorylation is visible, likely reflecting the low-level expression of endogenous ephrin-A in these cells (Nievergall et al., 2010) and explaining the low-level segregation that we observe when these two cell lines are cocultured (Fig. 6, A and B). In agreement, coculture of nontransfected parental HEK293T and EphA3/HEK293T cells resulted in similar EphA3 phosphorylation, whereas preclustered ephrin-B1-Fc was ineffective (Fig. S4).

The notion from cancer genome screens of function-impeding somatic EphA3 mutations (Ding et al., 2008) together with our findings prompted us to assess whether overexpression of kinase-dead EphA3 would also affect ephrin-B1/EphB2–mediated cell sorting in a dominant-negative manner. Thus, we compared cell segregation by GFP-EphB2/HEK293T cells (Jørgensen et al., 2009) transfected with Wt or mutant EphA3[K653M] and isolated for EphA3 expression by FACS with Alexa Fluor 594 IIIA4. Although coexpression of Wt EphA3 had no significant effect on the segregation capacity of GFP-EphB2, strikingly, coexpression of EphA3[K653M] in EphB2/GFP-expressing cells effectively inhibited their segregation from ephrin-B1 cells (Fig. 7, A and B), demonstrating that abundance of the kinase-inactive EphA receptor attenuates signaling and biological responses of ephrin-activated EphB receptors.

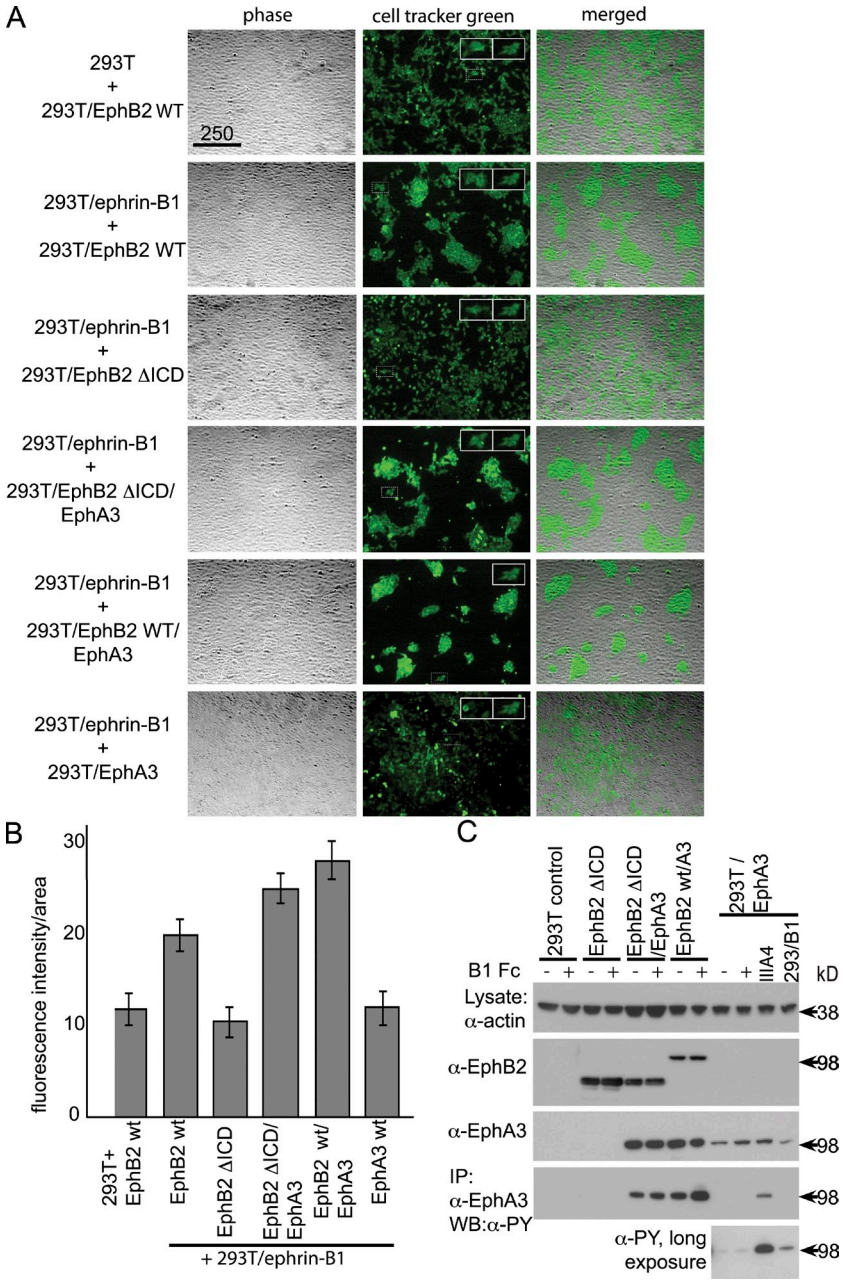

Figure 6. **EphA3 rescues defective cell segregation of EphB2ΔICD cells from ephrin-B1 cells.** (A) Ephrin-B1 HEK293 cells were cocultured with CellTracker green–labeled HEK293 cells expressing the indicated combinations of Wt or truncated EphB2 (ΔICD) and EphA3. At confluency (2–3 d), cells were fixed and imaged by phase-contrast and fluorescence microscopy. The scale bar shown is in micrometers. (B) Segregation of green-labeled and nonlabeled HEK293T cells was determined by measuring the tightness of (green) HEK293 cell aggregation and quantified by estimating mean fluorescence intensity per total fluorescence area (>12 random fields/condition). To illustrate equal fluorescence intensity of CellTracker green–labeled cells, insets in A illustrate comparisons of individual nonclustered cells (magnified from areas defined by dashed boxes) with those selected from the coculture of ephrin-B1/HEK293T and (green) Wt EphB2/EphA3 cells with maximal cell segregation. Statistical relevance of observed differences between all groups was determined using the analysis of variance (ANOVA) test for multiple comparisons. Means with error bars indicating 95% confidence intervals (ANOVA) are shown. (C) EphA3 is activated in response to ephrin-B1-Fc in Wt EphB2 and EphB2[ΔICD]-coexpressing cells but not in cells lacking EphB2. HEK293T cell lines illustrated in A were analyzed for EphA3 phosphorylation in response to cross-linked ephrin-B1-Fc by analyzing α-EphA3 IPs by an α-PY WB. To test ephrin-B1 stimulation of EphA3, EphA3/HEK293T cells were incubated with ephrin-B1-Fc, IIIA4 (positive control), or ephrinB1/293 cells. To control loading, lysates were blotted for EphA3 and EphB2 levels.

Discussion

Upon contact with ephrin-expressing cells, Eph receptors elicit cellular signaling and biological outcomes by assembly of oligomeric signaling clusters; compelling experimental evidence over the past decade attests that it is the sum of Ephs on a given cell competing for available ephrins on interacting cells, which determines the cellular response (Brown et al., 2000; Reber et al., 2004), typically adhesion or segregation between the interacting cells (Davy and Soriano, 2005; Pasquale, 2005; Egea and Klein, 2007). In recognition of the two Eph/ephrin specificity subclasses (Gale et al., 1996; Pasquale, 2004), it has been generally assumed that individual signaling clusters comprise Eph receptors, which are competent to interact with the corresponding ephrins. Indeed, ephrin-Fc or ephrin–alkaline phosphatase fusion proteins have been used to define the Eph/ephrin specificity subclasses (Gale et al., 1996; Pasquale, 2004) through interaction with relevant Eph family members (Cheng et al., 1995; Gale et al., 1996; Compagni et al., 2003; Marquardt et al., 2005).

Recently, global phosphoproteomic analysis of interacting EphB2- and ephrin-B1–expressing HEK293 cells suggested coincident regulation of EphA receptors in EphB2-activated cells (Jørgensen et al., 2009). We now demonstrate for the first time that A- and B-type Ephs, when coexpressed in the same cell, directly associate with each other in a common signaling complex. Accordingly, the recruitment of Eph receptors into a signaling cluster can occur independent of the ephrin specificity and is mediated by Eph–Eph interactions. As a consequence, the coexpression of Eph family members, even those that are

unable to bind the ligand on the interacting cell, can modulate signaling and biological responses of other Eph receptors engaged in ephrin interactions.

During embryogenesis, several Eph and ephrin family members are coexpressed within interacting cell populations (Lemke and Reber, 2005; Lackmann and Boyd, 2008; Pasquale, 2010) and on individual cells (Marquardt et al., 2005). Genetic studies indicate, for example, that during axonal path finding, multiple overlapping Eph expression gradients and their combined signaling control axon branching and final growth cone position (Reber et al., 2004; McLaughlin and O'Leary, 2005; Flanagan, 2006). Not surprisingly, tumors and tumor cell lines also frequently coexpress several Eph and ephrin family members (Hafner et al., 2004, 2006; Herath et al., 2006; Alonso-C et al., 2009), and mounting evidence suggests that Eph signaling and the resulting cell biological responses triggered by interacting ephrins are defined by the sum of cell surface–expressed receptors of the corresponding subtype (Pasquale, 2010). A recent study suggests that in prostate carcinoma cells, coexpressed EphA and -B receptors generate disparate responses to ephrin contact, whereby EphB signaling promotes unhindered migration, whereas EphA signaling mediates contact-inhibited migration toward ephrin-expressing cells (Astin et al., 2010). In view of the Eph/ephrin subclass specificity, it was proposed that preferential activation of either EphA or EphB receptors and their signaling from distinct EphA and EphB clusters will dictate the response of these cells to interacting ephrin-expressing cells. We have now explored the possibility that A- and B-type Ephs directly associate and participate in a common signaling cluster that elicits cellular responses according to its composition from both receptors.

Previously, functional analysis of Eph/ephrin signal cluster assembly revealed that propagation of nascent signaling clusters could occur independent of ephrin contacts and cytosolic Eph signaling functions via direct Eph–Eph interactions (Lackmann et al., 1998; Wimmer-Kleikamp et al., 2004). Recent crystal structures defined the involved molecular interfaces within the globular and cysteine-rich Eph receptor domains (Himanen et al., 2010; Seiradake et al., 2010), but these studies did not explore whether the same mechanism may also heterooligomerize EphA and EphB receptors. We now confirm in prostate carcinoma and in glioma cell lines with endogenous EphA and EphB coexpression and in EphA3/EphB2 coexpressing HEK293 and COS7 cells used as in vitro models that constitutive association of two receptor subtypes is increased upon selective clustering of only one of the two receptors. We used confocal microscopy and FLIM to assess the association of EphA and EphB receptors and the proximity of their interaction in intact cells. In FLIM, FRET attenuation of donor fluorescent lifetimes depends on the proximity of interacting fluorophores within 10 nm (Wouters et al., 2001; Jares-Erijman and Jovin, 2003), and substantially reduced donor fluorescent lifetimes determined in our experiments indeed suggest very close and potentially direct interactions between the GFP and diHcRed-tagged Eph receptors. This notion is supported by our functional analysis, strongly suggesting that the Eph receptor kinase domains are in sufficient close juxtaposition to allow

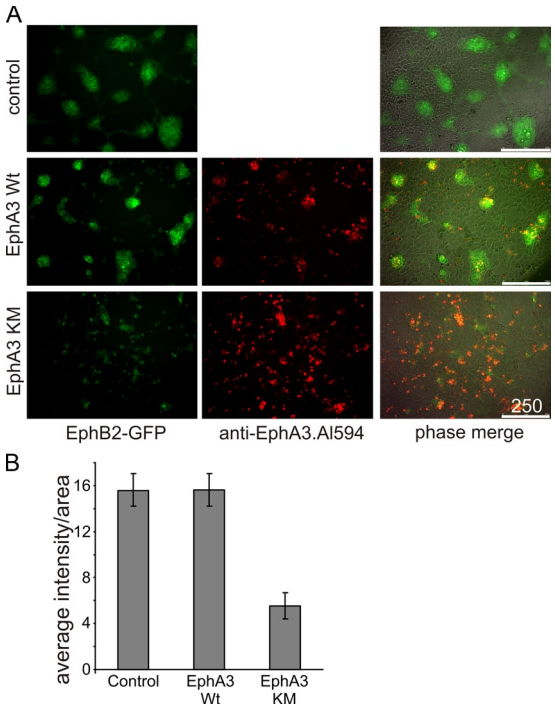

Figure 7. **Overexpression of kinase-inactive EphA3 causes dominant-negative inhibition of ephrin-B1/EphB2–mediated cell segregation.** (A) GFP-EphB2/HEK293 cells, transfected with Wt or EphA3[KM], were stained with Alexa Fluor 594 α-EphA3 mAb and enriched by FACS. Transfected or control GFP-EphB2/HEK293T cells were cocultured with ephrin-B1/HEK293T cells until confluent before imaging by fluorescence microscopy. All scale bars are in micrometers. (B) Segregation of GFP-EphB2/HEK293T and ephrin-B1/HEK293T cells was quantified as in Fig. 6 (10 random fields/condition). The graph shows means with error bars indicating 95% confidence intervals (ANOVA test for multiple comparisons).

transphosphorylation to occur. Thus, mutant EphA3[K653M] lacks kinase activity and phosphorylated tyrosines when expressed on its own. In the presence of coexpressed EphB2 and the EphA3 agonist IIIA4, it becomes tyrosine phosphorylated and effectively triggers cell contraction and cell–cell segregation, suggesting a tight functional complex between the EphA and EphB receptors.

Clearly, our investigation required an Eph agonist that, unlike ephrins, binds only one of the interacting Ephs; the α-EphA3 mAb IIIA4, which binds and exclusively activates EphA3 (Vearing et al., 2005), allowed the unambiguous detection of corecruitment and cross-activation of nonligated receptors. A previous mutagenesis screen mapped the IIIA4-binding site adjacent to the postulated low-affinity EphA3/ephrin-A5 heterodimerization interface, which is thought to link two high-affinity Eph/ephrin heterodimers into the heterotetrameric complex that promotes Eph/Eph oligomerization and effective Eph signaling (Smith et al., 2004). Recent crystal structures of EphA2–ephrin-A5 or –ephrin-A1 complexes (Himanen et al., 2010; Seiradake et al., 2010) confirmed these protein interfaces, suggesting that IIIA4 mimics the role of ephrin-A5-Fc by tethering two EphA3 receptors via their heterotetramerization sites to promote oligomerization (Vearing et al., 2005). In addition to these prominent interfaces facilitating Eph clustering, models derived from Eph crystal structures suggest a

potential contribution also of the N-terminal fibronectin type III (FNIII) motif to the Eph–Eph interface, although functional evidence for this interaction is lacking. Indeed, almost complete loss of heteroclustering between EphB2 and EphA2/3 LBD mutants in our experiments would seem to confirm the dominating role proposed for these particular domains to the clustering interface (Himanen et al., 2010).

Interestingly, selective biotinylation and subsequent clustering and activation with SA beads of biotinylated AP-EphB2 also trigger activation/phosphorylation, as was initially shown for EphA3 (Howarth and Ting, 2008; Nievergall et al., 2010), in which localized clustering of biotinylated EphA3 onto SA beads allowed detecting the recruitment of the ER-bound phosphatase PTP1B into cell surface EphA3 signaling clusters (Nievergall et al., 2010). In our current study, the same approach unambiguously revealed that EphB2 is recruited, independent of interaction with ephrins, into the EphA3 cell surface cluster. A recent study suggests that to further the contribution of Eph–Eph clustering mechanisms previously described (Wimmer-Kleikamp et al., 2004) and in the current study, Eph-modulated actomyosin contractile forces may potentially participate in assembly and lateral expansion of Eph clusters, providing a positive feedback loop during Eph activation (Salaita et al., 2010). The involvement of such a mechanism would explain why in our experiments cytoplasmic truncation of EphA3 also weakly attenuates the association with EphB2.

Conceptually, it may seem to make little difference to the biological response if functionally distinct EphA and EphB receptors contribute from separate or shared signaling clusters, considering that some of the downstream signaling components will be shared (Pasquale, 2005), and, invariably, the abundance of one receptor type will dictate the overall response to ephrin contact. However, previous models considered that distinct EphA and EphB signaling clusters are only activated if ephrins binding to corresponding subclasses are present on the interacting cells (Lemke and Reber, 2005; Lackmann and Boyd, 2008; Pasquale, 2010). Our findings now suggest that even in the absence of ephrins with specificity for one of the Eph subtypes, the recruitment and functional association of EphA and EphB receptors within the common complex lead to signaling outcomes that reflect composite Eph clusters, potentially containing both Eph subclasses. Importantly, depending on the ratio between Wt and mutant Eph family members expressed in a cell, kinase-inactivating mutations of one Eph are either rescued by transphosphorylation or exert a dominant-negative effect on the Wt receptor. Thus, coexpression of moderate levels of kinase-defective EphA3 in COS7 cells with endogenous EphB2 expression results in its transphosphorylation by EphB2 and renders these cells responsive to cell contraction by the agonistic IIIA4 antibody. On the other hand, highly elevated expression of the kinase-defective EphA3 modulates signaling from the Eph cluster in a dominant-negative manner by strongly attenuating EphB2 phosphorylation, cell rounding, and segregation from ephrin-B1 cells.

A prominent example for a kinase-defective Eph receptor modulating signaling outcomes of its Wt parent is EphA7, directing the migration of neural fold cells during mouse development; increasing coexpression of cytoplasmic-truncated splice variants changes the response to ephrin-A5–expressing cells from repulsion to adhesion to facilitate effective closure of the neural tube (Holmberg et al., 2000). Whereas in this case a dose-dependent dominant-negative effect was shown to inhibit activation and reverse Wt EphA7 function, in other examples, the underlying signaling mechanisms are less well defined, and kinase-independent Eph functions have been postulated. For example, analysis of EphA8-triggered adhesion via β1 or β3 integrins in transfected NIH3T3 or HEK293 cells suggested a phosphatidylinositol 3-kinase (PI3K)-dependent mechanism that is independent of EphA8 kinase activity but is reliant on the presence of the EphA8 extracellular and juxtamembrane domains (Gu and Park, 2001). Likewise, a role of kinase-defective EphB6 in cell adhesion and migration was examined by transfection of HEK293T cells, revealing enhanced adhesion and migration at low, but repulsion and attenuated cell migration at high, ephrin-B2 concentrations (Matsuoka et al., 2005), whereas tyrosine phosphorylation and loss of cell adhesion in HEK293T cells overexpressing ephrin binding–compromised EphB4 were considered to reflect ephrin-independent EphB4 tumor cell functions (Noren et al., 2009). Also, in PC3 cells, transfection with mutant EphA2 revealed EphA2 kinase-independent effects on cell migration and invasion (Taddei et al., 2009). Considering our finding of coassociation and crosstalk between different Ephs, it would seem possible that endogenous expression of other Eph receptors, including EphA3 in HEK293 cells (Dottori et al., 1999) and EphB2 in PC3 cells (Astin et al., 2010), may have contributed to the signaling outcomes in these cells.

Given the high frequency of somatic cancer mutations in the genes of Eph receptors, in particular EphA3, which are likely to effect receptor clustering or kinase activity (Sjöblom et al., 2006; Ding et al., 2008), the contrary contributions of either low- or high-expressed kinase-defective Eph receptors to Eph-controlled cell–cell adhesion will undeniable have important functional relevance. Of note, the molecular switch between adhesive and de-adhesive responses to Eph-ephrin ligation is provided by distinct configurations of the active or inactive Eph kinase domain–controlling ADAM10-mediated ephrin cleavage and Eph endocytosis (Janes et al., 2009). A kinase-dead nonphosphorylated Eph remains bound to cell surface ephrins, is not endocytosed (Janes et al., 2009; Nievergall et al., 2010), and promotes stable cell–cell contacts. Thus, occurrence of Eph kinase–inactivating mutations cannot be considered as a loss of function analogous to a loss of protein expression but as a mechanism that switches the response to neighboring ephrin-expressing cells from cell–cell segregation to cell–cell adhesion and intermingling (Lackmann and Boyd, 2008). Our finding of crosstalk between Eph family members potentially relaying this reversal of response to ephrin contact across the combined Eph population on a cell has considerable implications for the understanding of Eph functions in cancer. It suggests that one may need to consider overall Eph family expression profiles rather than individual family members when examining the biological responses that are controlled by these cell guidance receptors.

Materials and methods

Expression constructs

A parental pEFBos EphA3 expression plasmid comprising the cDNA-encoding residues 1–983 of human EphA3 cloned into the pEF-BOS vector under control of the human EF-1α promoter (Lackmann et al., 1998) was used for construction of EphA3-GFP (Wimmer-Kleikamp et al., 2004), EphA3-YFP (Nievergall et al., 2010), and EphA3-diHcRed (Janes et al., 2005). EphA3 tagged with a biotin AP or Avi-tag (EphA3-AP; Janes et al., 2009) was used for making deletion mutants lacking the LBD (lacking residues 44–211) or CRD (residues 212–335) by insertion of BstZ17I restriction sites using site-directed mutagenesis (Agilent Technologies) and religation. Intracellular deletion was performed by insertion of a stop codon at Tyr570. GFP-tagged EphA2 extracellular domain, generated by cloning full-length human EphA2 from a Mammalian Gene Collection cDNA template into pEGFP-N2 (Invitrogen), was used to generate EphA2 extracellular domain deletion mutants lacking residues 28–198 (ΔLBD) or replacing residues 201–325 (ΔCRD) with a Gly-Ser-Gly-Ser linker by PCR-based cloning strategies, as previously described (Himanen et al., 2010). Mouse EphB2-GFP was generated within the mammalian expression vector pcDNA3 by inserting the GFP cDNA in between C-terminal residues Arg983 and Ala984 of EphB2, as previously described (Tong et al., 2003). From this vector, we generated EphB2 3YF using site-directed mutagenesis to alter Tyr604, -610, and -667 into Phe. EphB2-AP was made by insertional site-directed mutagenesis of the AP tag sequence after Val19 of the mouse EphB2 signal sequence, as previously described for EphA3 (Janes et al., 2009).

Reagents and antibodies

Ephrin-A5-Fc was produced in a CHO cell clone containing a mammalian plgBos cDNA expression plasmid in which the full-length ephrin-A5 (residues 1–228) in pBluescript is fused to the hinge and CH2 and CH3 regions of human IgG1; the ephrin-A5-Fc fusion protein was purified from the cell supernatants by successive protein A affinity chromatography and size-exclusion HPLC. Ephrin-B1-Fc, generated by a similar strategy, was provided by J. Himanen (Memorial Sloan-Kettering Cancer Center, New York, NY) and has been previously described (Lawrenson et al., 2002). Properties of the activating EphA3-specific mAb (clone IIIA4; Vearing et al., 2005) and the EphA3 sheep pAb used for immunoblots (Nievergall et al., 2010) have been previously described. Commercially available antibodies were used for EphB2 (pAb; R&D Systems), phospho-EphA3 (pAb; Millipore), PY (pAb; Invitrogen), GFP (mAb; Roche), and the AP tag (Avi-tag pAb; GenScript). SA M-280 Dynabeads and protein A Dynabeads were obtained from Invitrogen. Alexa Fluor–labeled SA and secondary antibodies were obtained from Molecular Probes, as were kits for Alexa Fluor labeling of IIIA4 mAb. Immunoprecipitation of antibody-bound proteins was with protein A Sepharose (CL4B; GE Healthcare), except for EphA3, for which IIIA4-coupled Mini-Leak beads (Vearing et al., 2005) were used (Kem-En-Tec Diagnostics).

Cell culture and biochemical analysis

HEK293, COS7, and U251 glioma and PC3, DU145, and LNCaP prostate cancer cell lines were obtained from the American Type Culture Collection and maintained in DME, 10% FCS, and 2 mM L-Glutamine in 5% CO_2. Stably transfected HEK293 cells expressing ephrin-B1 or coexpressing EphB2 with membrane-targeted GFP (gapGFP) were provided by D. Wilkinson and A. Poliakov (Medical Research Council National Institute for Medical Research, London, England, UK; Poliakov et al., 2008) and were maintained in the presence of 200 µg/ml G418. EphB2 lacking the cytoplasmic domain (EphB2ΔICD) was generated by stably transfecting HEK293 cells with a mammalian expression construct for cytoplasmic-truncated EphB2 (Poliakov et al., 2008), using G418 for selection. Expression levels in these cells were tested by immunoblotting of cell lysates, immunofluorescence, and FACS, as previously described (Jørgensen et al., 2009). HEK293 and COS7 cells stably expressing EphA3 Wt or inactive mutant EphA3[KM] were generated by antibiotic selection with 200 µg/ml Zeocin (Invitrogen).

Stimulation of cells was performed with ephrin-A5-Fc or ephrin-B1-Fc (1.5 µg/ml final) preclustered using anti–human IgG (0.75 µg/ml Fc-γ specific; Jackson ImmunoResearch Laboratories, Inc.) or IIIA4 (1.5 µg/ml final) preclustered using anti–mouse IgG, typically for 15 min. Whole-cell lysis was performed in 50 mM Tris, pH 7.4, 150 mM NaCl, 1% Triton X-100, 0.1% SDS, 1 mM $NaV0_4$, 10 mM NaF, and protease inhibitors (Complete; Roche). IPs or whole-cell lysates were analyzed by SDS-PAGE on 4–12% Bis-Tris gels (BioRad Laboratories or Invitrogen), and WBs were visualized using HRP-coupled secondary antibodies (Jackson ImmunoResearch Laboratories, Inc.) and an ECL substrate (SuperSignal; Thermo Fisher Scientific).

Quantitative PCR analysis of glioma tissue

Primary specimens were obtained from the Royal Brisbane and Women's Hospital and the Briz Brain and Spine Research Foundation after informed consent from adult patients diagnosed with high-grade glioma. RNA was extracted using TRIZOL (Invitrogen). First-strand cDNA was synthesized using random hexamers and Superscript III (Invitrogen). Real-time PCR was performed using SYBR green PCR Master Mix (Applied Biosystems). Cycling conditions were 15 min at 95°C and 30 cycles of 30 s at 95°C, 30 s at 55°C, and 30 s at 72°C.

Confocal and fluorescence microscopy analysis

Confocal microscopy was performed with a microscope (FluoView 1000; Olympus) equipped with 488-nm argon, 543-nm helium–neon, and 633-nm helium–neon lasers using an oil immersion 60× objective lens (1.4 NA). Cells were plated into fibronectin-treated coverslips, transfected, and stained as indicated. Images were analyzed with analySIS software (Soft Imaging System), and merging of micrographs from individual fluorescent channels (Figs. 2 and S3) was performed in Photoshop (Adobe).

FLIM sequences were obtained at a modulation frequency of 80 MHz with a microscope (IX70; Olympus) using a 100×/1.4 NA oil objective. EYFP was excited with the 514-nm line of an argon ion laser. The acceptor fluorophore diHcRed was imaged using a 100-W mercury arc lamp and a Texas red filter set. FLIM data were processed using IPLab software (Scanalytics) and a custom-designed script, as previously described (Verveer et al., 2000). Fluorescence lifetime images are presented in pseudocolor. Images show YFP fluorescence phase-modulation lifetimes. Imaging of cells for retraction and segregation assays was performed on an imaging system (AF6000 LX; Leica) equipped with N Plan 20× (0.35 NA) and FLUOstar 40× (0.6 NA) dry objectives using time-lapse and multipoint positioning functions.

Cell retraction and segregation assays

Eph-mediated cell retraction was assayed using COS7 cells plated into 8-well chamber slides (BD) precoated with 10 µg/ml fibronectin. Cells were prestained on ice with 5 µg/ml Alexa Fluor 594–labeled anti-EphA3 (IIIA4) antibody, washed once, and imaged by time lapse after an addition of 0.75 µg/ml anti–mouse IgG to cross-link the antibody-bound receptors.

Cell segregation assays were performed essentially as previously described (Poliakov et al., 2008). In brief, a total of 60,000 cells/well containing labeled and nonlabeled Eph and ephrin-expressing cells, as indicated, was seeded into fibronectin-precoated 8-well chamber slides (BD) and incubated for 2 d or until confluent. Where indicated, one cell population was prelabeled with CellTracker green (Invitrogen), as per the manufacturer's instructions. Images were taken at identical settings and analyzed with ImageJ software (National Institutes of Health) to determine fluorescence intensity (green channel) divided by the area of fluorescence as a measure of tightness of segregation of the two cell populations. Merging of fluorescent and brightfield micrographs was performed in Photoshop.

Online supplemental material

Fig. S1 shows expression of individual receptors or combined subsets of EphA and EphB receptors in glioma patient tumor tissue samples. Fig. S2 shows analysis by IP/WB of EphA and EphB receptor coassociation and cross-phosphorylation in tumor cell lines. Fig. S3 illustrates the association between EphA3 and EphB2 by confocal microscopy, IP, and FRET analysis. Fig. S4 shows IP/WB analysis revealing that EphA3 is not activated by ephrin-B1-Fc but is slightly activated by coincubation with HEK293 cells. Video 1 shows a time lapse of Alexa Fluor 594 IIIA4–induced contraction of a Wt EphA3–transfected COS7 cell. Video 2 illustrates Alexa Fluor 594 IIIA4–induced contraction of an EphA3[KM]-transfected COS7 cell. Video 3 shows that time-lapse microscopy of a group of Wt EphA3–expressing COS7 cells reveals ephrin-B1–induced cell contraction. Video 4 shows ephrin-B1–induced cell contraction of a Wt EphA3–expressing COS7 cell. Video 5 illustrates time-lapse microscopy of COS7 cells overexpressing signaling-defective EphA3[KM], which do not respond to ephrin-B1-Fc exposure with contraction. Video 6 reveals limited ephrin-B1-Fc–induced contraction of a single COS7 cell with low EphA3[KM] expression among a group of EphA3[KM]-overexpressing COS7 cells.

We thank Juha Himanen and Dimitar Nikolov for providing ephrin-B1-Fc, Andrew Scott, Angelo Peroni, and Benjamin Gloria for IIIA4 antibody production, and David Wilkinson and Alexi Poliakov for providing 293/ephrin-B1 and

293/EphB2 cells coexpressing membrane-targeted GFP. We are grateful to the Monash Micro Imaging staff for microscopy advice and the Monash FlowCore facility for FACS.

This work was supported by grants from the Human Frontier Science Program (RGP0039/2009-C), the National Health and Medical Research Council of Australia (334085 and 487922), and National Health and Medical Research Council RD Wright and Senior Research fellowships to P.W. Janes and M. Lackmann.

Submitted: 8 April 2011
Accepted: 3 November 2011

References

Alonso-C, L.M., E.M. Trinidad, B. de Garcillan, M. Ballesteros, M. Castellanos, I. Cotillo, J.J. Muñoz, and A.G. Zapata. 2009. Expression profile of Eph receptors and ephrin ligands in healthy human B lymphocytes and chronic lymphocytic leukemia B-cells. *Leuk. Res.* 33:395–406. http://dx.doi.org/10.1016/j.leukres.2008.08.010

Astin, J.W., J. Batson, S. Kadir, J. Charlet, R.A. Persad, D. Gillatt, J.D. Oxley, and C.D. Nobes. 2010. Competition amongst Eph receptors regulates contact inhibition of locomotion and invasiveness in prostate cancer cells. *Nat. Cell Biol.* 12:1194–1204. http://dx.doi.org/10.1038/ncb2122

Batlle, E., J. Bacani, H. Begthel, S. Jonkheer, A. Gregorieff, M. van de Born, N. Malats, E. Sancho, E. Boon, T. Pawson, et al. 2005. EphB receptor activity suppresses colorectal cancer progression. *Nature*. 435:1126–1130. http://dx.doi.org/10.1038/nature03626

Binns, K.L., P.P. Taylor, F. Sicheri, T. Pawson, and S.J. Holland. 2000. Phosphorylation of tyrosine residues in the kinase domain and juxtamembrane region regulates the biological and catalytic activities of Eph receptors. *Mol. Cell. Biol.* 20:4791–4805. http://dx.doi.org/10.1128/MCB.20.13.4791-4805.2000

Brown, A., P.A. Yates, P. Burrola, D. Ortuño, A. Vaidya, T.M. Jessell, S.L. Pfaff, D.D. O'Leary, and G. Lemke. 2000. Topographic mapping from the retina to the midbrain is controlled by relative but not absolute levels of EphA receptor signaling. *Cell*. 102:77–88. http://dx.doi.org/10.1016/S0092-8674(00)00012-X

Cheng, H.J., M. Nakamoto, A.D. Bergemann, and J.G. Flanagan. 1995. Complementary gradients in expression and binding of ELF-1 and Mek4 in development of the topographic retinotectal projection map. *Cell*. 82:371–381. http://dx.doi.org/10.1016/0092-8674(95)90426-3

Clevers, H., and E. Batlle. 2006. EphB/EphrinB receptors and Wnt signaling in colorectal cancer. *Cancer Res.* 66:2–5. http://dx.doi.org/10.1158/0008-5472.CAN-05-3849

Compagni, A., M. Logan, R. Klein, and R.H. Adams. 2003. Control of skeletal patterning by ephrinB1-EphB interactions. *Dev. Cell*. 5:217–230. http://dx.doi.org/10.1016/S1534-5807(03)00198-9

Cortina, C., S. Palomo-Ponce, M. Iglesias, J.L. Fernández-Masip, A. Vivancos, G. Whissell, M. Humà, N. Peiró, L. Gallego, S. Jonkheer, et al. 2007. EphB-ephrin-B interactions suppress colorectal cancer progression by compartmentalizing tumor cells. *Nat. Genet.* 39:1376–1383. http://dx.doi.org/10.1038/ng.2007.11

Davis, S., N.W. Gale, T.H. Aldrich, P.C. Maisonpierre, V. Lhotak, T. Pawson, M. Goldfarb, and G.D. Yancopoulos. 1994. Ligands for EPH-related receptor tyrosine kinases that require membrane attachment or clustering for activity. *Science*. 266:816–819. http://dx.doi.org/10.1126/science.7973638

Davy, A., and P. Soriano. 2005. Ephrin signaling in vivo: Look both ways. *Dev. Dyn.* 232:1–10. http://dx.doi.org/10.1002/dvdy.20200

Ding, L., G. Getz, D.A. Wheeler, E.R. Mardis, M.D. McLellan, K. Cibulskis, C. Sougnez, H. Greulich, D.M. Muzny, M.B. Morgan, et al. 2008. Somatic mutations affect key pathways in lung adenocarcinoma. *Nature*. 455:1069–1075. http://dx.doi.org/10.1038/nature07423

Dottori, M., M. Down, A. Hüttmann, D.R. Fitzpatrick, and A.W. Boyd. 1999. Cloning and characterization of EphA3 (Hek) gene promoter: DNA methylation regulates expression in hematopoietic tumor cells. *Blood*. 94:2477–2486.

Egea, J., and R. Klein. 2007. Bidirectional Eph-ephrin signaling during axon guidance. *Trends Cell Biol.* 17:230–238. http://dx.doi.org/10.1016/j.tcb.2007.03.004

Flanagan, J.G. 2006. Neural map specification by gradients. *Curr. Opin. Neurobiol.* 16:59–66. http://dx.doi.org/10.1016/j.conb.2006.01.010

Freywald, A., N. Sharfe, and C.M. Roifman. 2002. The kinase-null EphB6 receptor undergoes transphosphorylation in a complex with EphB1. *J. Biol. Chem.* 277:3823–3828. http://dx.doi.org/10.1074/jbc.M108011200

Gale, N.W., S.J. Holland, D.M. Valenzuela, A. Flenniken, L. Pan, T.E. Ryan, M. Henkemeyer, K. Strebhardt, H. Hirai, D.G. Wilkinson, et al. 1996. Eph receptors and ligands comprise two major specificity subclasses and are reciprocally compartmentalized during embryogenesis. *Neuron*. 17:9–19. http://dx.doi.org/10.1016/S0896-6273(00)80276-7

Gu, C., and S. Park. 2001. The EphA8 receptor regulates integrin activity through p110gamma phosphatidylinositol-3 kinase in a tyrosine kinase activity-independent manner. *Mol. Cell. Biol.* 21:4579–4597. http://dx.doi.org/10.1128/MCB.21.14.4579-4597.2001

Hafner, C., G. Schmitz, S. Meyer, F. Bataille, P. Hau, T. Langmann, W. Dietmaier, M. Landthaler, and T. Vogt. 2004. Differential gene expression of Eph receptors and ephrins in benign human tissues and cancers. *Clin. Chem.* 50:490–499. http://dx.doi.org/10.1373/clinchem.2003.026849

Hafner, C., B. Becker, M. Landthaler, and T. Vogt. 2006. Expression profile of Eph receptors and ephrin ligands in human skin and downregulation of EphA1 in nonmelanoma skin cancer. *Mod. Pathol.* 19:1369–1377. http://dx.doi.org/10.1038/modpathol.3800660

Herath, N.I., M.D. Spanevello, S. Sabesan, T. Newton, M. Cummings, S. Duffy, D. Lincoln, G. Boyle, P.G. Parsons, and A.W. Boyd. 2006. Over-expression of Eph and ephrin genes in advanced ovarian cancer: Ephrin gene expression correlates with shortened survival. *BMC Cancer*. 6:144. http://dx.doi.org/10.1186/1471-2407-6-144

Himanen, J.P., M.J. Chumley, M. Lackmann, C. Li, W.A. Barton, P.D. Jeffrey, C. Vearing, D. Geleick, D.A. Feldheim, A.W. Boyd, et al. 2004. Repelling class discrimination: Ephrin-A5 binds to and activates EphB2 receptor signaling. *Nat. Neurosci.* 7:501–509. http://dx.doi.org/10.1038/nn1237

Himanen, J.P., L. Yermekbayeva, P.W. Janes, J.R. Walker, K. Xu, L. Atapattu, K.R. Rajashankar, A. Mensinga, M. Lackmann, D.B. Nikolov, and S. Dhe-Paganon. 2010. Architecture of Eph receptor clusters. *Proc. Natl. Acad. Sci. USA*. 107:10860–10865. http://dx.doi.org/10.1073/pnas.1004148107

Holmberg, J., and J. Frisén. 2002. Ephrins are not only unattractive. *Trends Neurosci.* 25:239–243. http://dx.doi.org/10.1016/S0166-2236(02)02149-5

Holmberg, J., D.L. Clarke, and J. Frisén. 2000. Regulation of repulsion versus adhesion by different splice forms of an Eph receptor. *Nature*. 408:203–206. http://dx.doi.org/10.1038/35041577

Howarth, M., and A.Y. Ting. 2008. Imaging proteins in live mammalian cells with biotin ligase and monovalent streptavidin. *Nat. Protoc.* 3:534–545. http://dx.doi.org/10.1038/nprot.2008.20

Howarth, M., K. Takao, Y. Hayashi, and A.Y. Ting. 2005. Targeting quantum dots to surface proteins in living cells with biotin ligase. *Proc. Natl. Acad. Sci. USA*. 102:7583–7588. http://dx.doi.org/10.1073/pnas.0503125102

Huusko, P., D. Ponciano-Jackson, M. Wolf, J.A. Kiefer, D.O. Azorsa, S. Tuzmen, D. Weaver, C. Robbins, T. Moses, M. Allinen, et al. 2004. Nonsense-mediated decay microarray analysis identifies mutations of EPHB2 in human prostate cancer. *Nat. Genet.* 36:979–983. http://dx.doi.org/10.1038/ng1408

Janes, P.W., N. Saha, W.A. Barton, M.V. Kolev, S.H. Wimmer-Kleikamp, E. Nievergall, C.P. Blobel, J.P. Himanen, M. Lackmann, and D.B. Nikolov. 2005. Adam meets Eph: An ADAM substrate recognition module acts as a molecular switch for ephrin cleavage in trans. *Cell*. 123:291–304. http://dx.doi.org/10.1016/j.cell.2005.08.014

Janes, P.W., S. Adikari, and M. Lackmann. 2008. Eph/ephrin signalling and function in oncogenesis: Lessons from embryonic development. *Curr. Cancer Drug Targets*. 8:473–479. http://dx.doi.org/10.2174/156800908785699315

Janes, P.W., S.H. Wimmer-Kleikamp, A.S. Frangakis, K. Treble, B. Griesshaber, O. Sabet, M. Grabenbauer, A.Y. Ting, P. Saftig, P.I. Bastiaens, and M. Lackmann. 2009. Cytoplasmic relaxation of active Eph controls ephrin shedding by ADAM10. *PLoS Biol.* 7:e1000215. http://dx.doi.org/10.1371/journal.pbio.1000215

Jares-Erijman, E.A., and T.M. Jovin. 2003. FRET imaging. *Nat. Biotechnol.* 21:1387–1395. http://dx.doi.org/10.1038/nbt896

Jørgensen, C., A. Sherman, G.I. Chen, A. Pasculescu, A. Poliakov, M. Hsiung, B. Larsen, D.G. Wilkinson, R. Linding, and T. Pawson. 2009. Cell-specific information processing in segregating populations of Eph receptor ephrin-expressing cells. *Science*. 326:1502–1509. http://dx.doi.org/10.1126/science.1176615

Klein, R. 2004. Eph/ephrin signaling in morphogenesis, neural development and plasticity. *Curr. Opin. Cell Biol.* 16:580–589. http://dx.doi.org/10.1016/j.ceb.2004.07.002

Koolpe, M., R. Burgess, M. Dail, and E.B. Pasquale. 2005. EphB receptor-binding peptides identified by phage display enable design of an antagonist with ephrin-like affinity. *J. Biol. Chem.* 280:17301–17311. http://dx.doi.org/10.1074/jbc.M500363200

Lackmann, M., and A.W. Boyd. 2008. Eph, a protein family coming of age: More confusion, insight, or complexity? *Sci. Signal.* 1:re2. http://dx.doi.org/10.1126/stke.115re2

Lackmann, M., R.J. Mann, L. Kravets, F.M. Smith, T.A. Bucci, K.F. Maxwell, G.J. Howlett, J.E. Olsson, T. Vanden Bos, D.P. Cerretti, and A.W. Boyd. 1997. Ligand for EPH-related kinase (LERK) 7 is the preferred high

affinity ligand for the HEK receptor. *J. Biol. Chem.* 272:16521–16530. http://dx.doi.org/10.1074/jbc.272.26.16521

Lackmann, M., A.C. Oates, M. Dottori, F.M. Smith, C. Do, M. Power, L. Kravets, and A.W. Boyd. 1998. Distinct subdomains of the EphA3 receptor mediate ligand binding and receptor dimerization. *J. Biol. Chem.* 273:20228–20237. http://dx.doi.org/10.1074/jbc.273.32.20228

Lawrenson, I.D., S.H. Wimmer-Kleikamp, P. Lock, S.M. Schoenwaelder, M. Down, A.W. Boyd, P.F. Alewood, and M. Lackmann. 2002. Ephrin-A5 induces rounding, blebbing and de-adhesion of EphA3-expressing 293T and melanoma cells by CrkII and Rho-mediated signalling. *J. Cell Sci.* 115:1059–1072.

Lemke, G., and M. Reber. 2005. Retinotectal mapping: New insights from molecular genetics. *Annu. Rev. Cell Dev. Biol.* 21:551–580. http://dx.doi.org/10.1146/annurev.cellbio.20.022403.093702

Marquardt, T., R. Shirasaki, S. Ghosh, S.E. Andrews, N. Carter, T. Hunter, and S.L. Pfaff. 2005. Coexpressed EphA receptors and ephrin-A ligands mediate opposing actions on growth cone navigation from distinct membrane domains. *Cell*. 121:127–139. http://dx.doi.org/10.1016/j.cell.2005.01.020

Matsuoka, H., H. Obama, M.L. Kelly, T. Matsui, and M. Nakamoto. 2005. Biphasic functions of the kinase-defective Ephb6 receptor in cell adhesion and migration. *J. Biol. Chem.* 280:29355–29363. http://dx.doi.org/10.1074/jbc.M500010200

McLaughlin, T., and D.D. O'Leary. 2005. Molecular gradients and development of retinotopic maps. *Annu. Rev. Neurosci.* 28:327–355. http://dx.doi.org/10.1146/annurev.neuro.28.061604.135714

Mellitzer, G., Q. Xu, and D.G. Wilkinson. 1999. Eph receptors and ephrins restrict cell intermingling and communication. *Nature*. 400:77–81. http://dx.doi.org/10.1038/21907

Nievergall, E., P.W. Janes, C. Stegmayer, M.E. Vail, F.G. Haj, S.W. Teng, B.G. Neel, P.I. Bastiaens, and M. Lackmann. 2010. PTP1B regulates Eph receptor function and trafficking. *J. Cell Biol.* 191:1189–1203. http://dx.doi.org/10.1083/jcb.201005035

Noren, N.K., G. Foos, C.A. Hauser, and E.B. Pasquale. 2006. The EphB4 receptor suppresses breast cancer cell tumorigenicity through an Abl-Crk pathway. *Nat. Cell Biol.* 8:815–825. http://dx.doi.org/10.1038/ncb1438

Noren, N.K., N.Y. Yang, M. Silldorff, R. Mutyala, and E.B. Pasquale. 2009. Ephrin-independent regulation of cell substrate adhesion by the EphB4 receptor. *Biochem. J.* 422:433–442. http://dx.doi.org/10.1042/BJ20090014

Pasquale, E.B. 2004. Eph-ephrin promiscuity is now crystal clear. *Nat. Neurosci.* 7:417–418. http://dx.doi.org/10.1038/nn0504-417

Pasquale, E.B. 2005. Eph receptor signalling casts a wide net on cell behaviour. *Nat. Rev. Mol. Cell Biol.* 6:462–475. http://dx.doi.org/10.1038/nrm1662

Pasquale, E.B. 2010. Eph receptors and ephrins in cancer: Bidirectional signalling and beyond. *Nat. Rev. Cancer.* 10:165–180. http://dx.doi.org/10.1038/nrc2806

Poliakov, A., M.L. Cotrina, A. Pasini, and D.G. Wilkinson. 2008. Regulation of EphB2 activation and cell repulsion by feedback control of the MAPK pathway. *J. Cell Biol.* 183:933–947. http://dx.doi.org/10.1083/jcb.200807151

Reber, M., P. Burrola, and G. Lemke. 2004. A relative signalling model for the formation of a topographic neural map. *Nature*. 431:847–853. http://dx.doi.org/10.1038/nature02957

Salaita, K., P.M. Nair, R.S. Petit, R.M. Neve, D. Das, J.W. Gray, and J.T. Groves. 2010. Restriction of receptor movement alters cellular response: Physical force sensing by EphA2. *Science*. 327:1380–1385. http://dx.doi.org/10.1126/science.1181729

Seiradake, E., K. Harlos, G. Sutton, A.R. Aricescu, and E.Y. Jones. 2010. An extracellular steric seeding mechanism for Eph-ephrin signaling platform assembly. *Nat. Struct. Mol. Biol.* 17:398–402. http://dx.doi.org/10.1038/nsmb.1782

Sjöblom, T., S. Jones, L.D. Wood, D.W. Parsons, J. Lin, T.D. Barber, D. Mandelker, R.J. Leary, J. Ptak, N. Silliman, et al. 2006. The consensus coding sequences of human breast and colorectal cancers. *Science*. 314:268–274. http://dx.doi.org/10.1126/science.1133427

Smith, F.M., C. Vearing, M. Lackmann, H. Treutlein, J. Himanen, K. Chen, A. Saul, D. Nikolov, and A.W. Boyd. 2004. Dissecting the EphA3/Ephrin-A5 interactions using a novel functional mutagenesis screen. *J. Biol. Chem.* 279:9522–9531. http://dx.doi.org/10.1074/jbc.M309326200

Stein, E., A.A. Lane, D.P. Cerretti, H.O. Schoecklmann, A.D. Schroff, R.L. Van Etten, and T.O. Daniel. 1998. Eph receptors discriminate specific ligand oligomers to determine alternative signaling complexes, attachment, and assembly responses. *Genes Dev.* 12:667–678. http://dx.doi.org/10.1101/gad.12.5.667

Taddei, M.L., M. Parri, A. Angelucci, B. Onnis, F. Bianchini, E. Giannoni, G. Raugei, L. Calorini, N. Rucci, A. Teti, et al. 2009. Kinase-dependent and -independent roles of EphA2 in the regulation of prostate cancer invasion and metastasis. *Am. J. Pathol.* 174:1492–1503. http://dx.doi.org/10.2353/ajpath.2009.080473

Tong, J., S. Elowe, P. Nash, and T. Pawson. 2003. Manipulation of EphB2 regulatory motifs and SH2 binding sites switches MAPK signaling and biological activity. *J. Biol. Chem.* 278:6111–6119. http://dx.doi.org/10.1074/jbc.M208972200

Vearing, C., F.T. Lee, S. Wimmer-Kleikamp, V. Spirkoska, C. To, C. Stylianou, M. Spanevello, M. Brechbiel, A.W. Boyd, A.M. Scott, and M. Lackmann. 2005. Concurrent binding of anti-EphA3 antibody and ephrin-A5 amplifies EphA3 signaling and downstream responses: Potential as EphA3-specific tumor-targeting reagents. *Cancer Res.* 65:6745–6754. http://dx.doi.org/10.1158/0008-5472.CAN-05-0758

Verveer, P.J., A. Squire, and P.I. Bastiaens. 2000. Global analysis of fluorescence lifetime imaging microscopy data. *Biophys. J.* 78:2127–2137. http://dx.doi.org/10.1016/S0006-3495(00)76759-2

Wimmer-Kleikamp, S.H., P.W. Janes, A. Squire, P.I.H. Bastiaens, and M. Lackmann. 2004. Recruitment of Eph receptors into signaling clusters does not require ephrin contact. *J. Cell Biol.* 164:661–666. http://dx.doi.org/10.1083/jcb.200312001

Wouters, F.S., P.J. Verveer, and P.I. Bastiaens. 2001. Imaging biochemistry inside cells. *Trends Cell Biol.* 11:203–211. http://dx.doi.org/10.1016/S0962-8924(01)01982-1

Wybenga-Groot, L.E., B. Baskin, S.H. Ong, J. Tong, T. Pawson, and F. Sicheri. 2001. Structural basis for autoinhibition of the Ephb2 receptor tyrosine kinase by the unphosphorylated juxtamembrane region. *Cell*. 106:745–757. http://dx.doi.org/10.1016/S0092-8674(01)00496-2

Xu, Q., G. Mellitzer, and D.G. Wilkinson. 2000. Roles of Eph receptors and ephrins in segmental patterning. *Philos. Trans. R. Soc. Lond. B Biol. Sci.* 355:993–1002. http://dx.doi.org/10.1098/rstb.2000.0635